Am J Physiol Renal Physiol 294: F554–F561, 2008.
First published December 26, 2007; doi:10.1152/ajprenal.00391.2007.

Inhibition of proinflammatory genes in anti-GBM glomerulonephritis by targeted dexamethasone-loaded Ab_{Esel} liposomes

Sigrídur A. Ásgeirsdóttir,[1] Peter J. Zwiers,[1] Henriëtte W. Morselt,[1] Hendrik E. Moorlag,[1] Hester I. Bakker,[1] Peter Heeringa,[1] Jan Willem Kok,[2] Cees G. M. Kallenberg,[3] Grietje Molema,[1] and Jan A. A. M. Kamps[1]

[1]*Department of Pathology and Laboratory Medicine, Medical Biology Section,* [2]*Department of Cell Biology, Section of Membrane Cell Biology, and* [3]*Department of Clinical Immunology, University Medical Center Groningen, University of Groningen, Groningen, The Netherlands*

Submitted 20 August 2007; accepted in final form 20 December 2007

Ásgeirsdóttir SA, Zwiers PJ, Morselt HW, Moorlag HE, Bakker HI, Heeringa P, Kok JW, Kallenberg CG, Molema G, Kamps JA. Inhibition of proinflammatory genes in anti-GBM glomerulonephritis by targeted dexamethasone-loaded Ab_{Esel} liposomes. *Am J Physiol Renal Physiol* 294: F554–F561, 2008. First published December 26, 2007; doi:10.1152/ajprenal.00391.2007.—E-selectin-directed targeted drug delivery was analyzed in anti-glomerular basement membrane glomerulonephritis. Liposomes conjugated with anti-E-selectin antibodies (Ab_{Esel} liposomes) were internalized by activated endothelial cells in vitro through E-selectin-mediated endocytosis. At the onset of glomerulonephritis in mice, E-selectin was expressed on glomerular endothelial cells, which resulted in homing of Ab_{Esel} liposomes to glomeruli after intravenous administration. Accumulation of Ab_{Esel} liposomes in the kidney was 3.6 times higher than nontargeted IgG liposomes, whereas the accumulation of both liposomes in the clearance organs liver and spleen and in heart and lungs was comparable. In glomeruli, the Ab_{Esel} liposomes colocalized with the endothelial cell marker CD31. Quantitative RT-PCR analysis of laser-microdissected arterioles, glomeruli, and postcapillary venules demonstrated that targeted delivery of dexamethasone by Ab_{Esel} liposomes reduced glomerular endothelial expression of P-selectin, E-selectin, and vascular cell adhesion molecule-1 by 60–70%. The expression of these genes was not modulated in endothelial cells in nontargeted renal microvasculatures. Decrease of glomerular endothelial activation at disease onset was followed by reduced albuminuria at *day 7*. This study demonstrates the potential of vascular bed-specific drug delivery aimed at disease-induced epitopes on the microvascular endothelial cells as a therapeutic strategy for glomerulonephritis.

glomerular endothelial cells; antiglomerular basement membrane disease; targeted interference; adhesion molecules; vascular gene expression

GLOMERULAR ENDOTHELIAL CELLS play an important role in fluid and solute filtration of the blood. Glomerular disorders result in glomerular injury leading to loss of renal functions. The onset of these diseases is characterized by triggering of proinflammatory pathways, including endothelial activation and glomerular influx of circulating leukocytes (12). The recruitment of leukocytes by activated endothelial cells is a well-orchestrated cascade of events via the processes of tethering and rolling, mediated by endothelial expression of P- and E-selectin, followed by firm adhesion through interaction between integrins on the leukocytes, and vascular cell adhesion molecule (VCAM)-1 and intercellular adhesion molecule-1 on endothelial cells (29).

Today many new potent anti-inflammatory drugs do not make it through clinical trials because of severe side effects (23). For these highly active drugs, a targeted delivery approach represents a significant added value for future clinical applicability. Liposomes are high-capacity drug carriers that, when modified with monoclonal antibodies, can be targeted to a target epitope of choice (17). For treatment of glomerulonephritis, glomerular endothelial cells are attractive targets for cell-specific drug delivery. Not only are they in direct contact with the bloodstream and hence well accessible for systemically administered therapeutics, but they also play a pivotal role in the pathological process associated with glomerulonephritis. Because E-selectin is uniquely restricted to activated endothelial cells (26) and is an internalizing receptor, it represents a suitable target for intracellular delivery of drugs that need to exert their pharmacological activity inside endothelial cells (10).

Our studies aimed at the development of a targeted liposomal delivery system capable of delivering drugs in glomerular endothelium. As a model drug, the corticosteroid dexamethasone was formulated in immunoliposomes, conjugated with anti-E-selectin antibodies (Ab_{Esel} liposomes), and its pharmacological activity was studied in antiglomerular basement membrane (anti-GBM) glomerulonephritis. Glucocorticoids are commonly used in anti-inflammatory therapy. Their most prominent pharmacological effect is inhibition of nuclear factor-κB and activator protein-1 driven expression of inflammatory genes encoding cytokines, receptors, and cell adhesion molecules (4). The pleiotropic clinical effects of glucocorticoids, however, can result in severe side effects, especially when given at higher doses and for longer periods (7, 28).

The current paper describes selective uptake of Ab_{Esel} liposomes into activated endothelial cells in vitro and into glomerular endothelium in vivo. Biodistribution of Ab_{Esel} liposomes and nontargeted IgG liposomes was established in mice suffering from accelerated glomerulonephritis. Pharmacological effects of targeted dexamethasone on the expression of proinflammatory genes were determined in glomeruli and endothelial cells in renal arterioles and postcapillary venules, and the pharmacological effects were compared with the effects of freely administrated dexamethasone.

Address for reprint requests and other correspondence: S. A. Ásgeirsdóttir, Dept. of Pathology & Laboratory Medicine, Medical Biology Section, Hanzeplein 1, 9713 GZ Groningen, The Netherlands (e-mail: s.a.asgeirsdottir@med.umcg.nl).

The costs of publication of this article were defrayed in part by the payment of page charges. The article must therefore be hereby marked "*advertisement*" in accordance with 18 U.S.C. Section 1734 solely to indicate this fact.

MATERIALS AND METHODS

Preparation of immunoliposomes. Synthesis of immunoliposomes was performed as described earlier (5, 18). Molar ratio of 1-palmitoyl-2-oleoyl-*sn*-glycero-3-phosphocholine (Avanti Polar Lipids, Alabaster, AL), cholesterol (Sigma-Aldrich, Zwijndrecht, The Netherlands), 1,2-distearoyl-*sn*-glycero-3-phosphoethanolamine-*N*-[methoxy(polyethylene glycol)-2000] (DSPE-PEG; Avanti Polar Lipids), and DSPE-PEG-maleimide (Avanti Polar Lipids) was 55:40:4:1. When indicated, liposomes contained 0.25 mol% lipid bilayer markers 1,1′-dioctadecyl-3,3,3′,3′-tetramethyl indocarbocyanine perchlorate (DiI; Molecular Probes, Eugene, OR) or a trace amount (0.25 μCi/μmol of total lipid) of [^{3}H]cholesteryloleyl ether (COE; GE Healthcare Europe, Diagem, Belgium). The lipids were hydrated in 10 mM HEPES and 135 mM NaCl, pH 6.7, or when appropriate in an aqueous solution of 75–100 mg/ml dexamethasone disodium phosphate (Bufa, Hilversum, The Netherlands). The monoclonal rat anti-mouse E-selectin antibody (MES-1, kindly provided by Dr. D. Brown, UCB Celltech, Slough, UK) and irrelevant rat IgG (Sigma-Aldrich) were thiolated by means of *N*-succinimidyl-*S*-acetylthioacetate (Sigma-Aldrich) and coupled to a maleimide group at the distal end of the polyethylene glycol chain by a sulfhydryl-maleimide coupling technique. The immunoliposomes were characterized by determining protein content using mouse IgG as a standard (24) and phospholipid phosphorus content (6). Total liposomal lipid concentration was adjusted for the amount of cholesterol present in the liposome preparations. Anti-E-selectin antibody (58 ± 18 μg/μmol lipid) and irrelevant rat IgG (75 ± 24 μg/μmol lipid) were coupled. Particle size was analyzed by dynamic light scattering using a Nicomp model 370 submicron particle analyzer (Santa Barbara, CA) in the volume-weighing model. The diameter size of Ab_{Esel} liposomes was 121 ± 20 nm and IgG liposomes 117 ± 15 nm. The content of encapsulated dexamethasone disodium-phosphate (Bufa) was determined after Bligh and Dyer extraction in the resulting methanol/H_2O phase by HPLC (21). Dexamethasone (55 ± 7 μg/μmol lipid) was encapsulated. Immunoliposomes were stored at 4°C and used within 3 wk after synthesis.

Endothelial cell cultures and in vitro experiments. The mouse endothelial cell line H5V (13) was kindly provided by Dr. A. Vecchi (Instituto Ricerche Farmacologische Mario Negri, Milan, Italy) and grown as previously described (11). Confluent monolayers were activated for 4 h with 100 ng/ml tumor necrosis factor (TNF)-α (Roche Diagnostics Nederland, Almere, The Netherlands). Cells were washed with cold PBS, trypsinized, and spun down on slides for immunohistochemical analysis. Cells were fixed in acetone for 10 min and incubated for 45 min with MES-1. After extensive washing with PBS, cytospots were incubated with horseradish peroxidase (HRP)-conjugated rabbit anti-rat IgG (DakoCytomation Denmark, Glostrup, Denmark). Counterstaining was performed with Mayers' hematoxylin (Klinipath, Duiven, The Netherlands), and slides were mounted with glycerin.

For in vitro binding studies, cells were grown in Lab-Tek chambers. $Alexa_{488}$-conjugated Ab_{Esel} (2 μg) or DiI-labeled Ab_{Esel} liposomes (40 nmol total lipid containing 2 μg Ab_{Esel}) were added to the medium 1 h after the start of activation with TNF-α. Where indicated, incubations were performed in the presence of 100 μg unlabeled antibodies for competition. Cells were washed with PBS and analyzed by fluorescence microscope (DM RXA; Leica Microsystems, Wetzlar, Germany) and Leica Q600 Qwin software V01.06.

Animals, glomerulonephritis model, Ab_{Esel}, and Ab_{Esel} liposome homing studies. C57bl/6 female mice were purchased from Harlan (Zeist, The Netherlands). Animals were maintained on mouse chow and tap water ad libitum in a temperature-controlled chamber at 24°C with a 12:12-h light-dark cycle. All animal experiments were performed according to national guidelines and upon approval of the local Animal Care and Use Committee of Groningen University.

Purification of polyclonal sheep anti-mouse GBM antibodies and induction of anti-GBM glomerulonephritis was performed as described previously (2). In short, immunization was initiated by 100 μl (2 mg/ml) commercially available sheep IgG (Sigma-Aldrich Chemie) mixed with 100 μl complete Freund's adjuvant (BD Pharmingen, Alphen aan den Rijn, The Netherlands) and injected intraperitoneally. After 6.5 days, glomerulonephritis was induced by intravenous injection with 1 mg sheep anti-mouse GBM antibodies and 200 ng recombinant mouse TNF-α (BioSource Europe, Nivelles, Belgium).

Ab_{Esel} antibodies and liposomes modified with Ab_{Esel} or IgG were injected at the onset of glomerulonephritis induction. Mice were killed at 2, 24, and 48 h later. Organs were perfused with ice-cold PBS, harvested, snap-frozen in liquid nitrogen, and stored at −80°C.

Cryosections (5 μm) were fixed in acetone for 10 min and incubated with fluorescein isothiocyanate-labeled rabbit anti-sheep IgG antibodies (DakoCytomation Denmark). Sections were examined using a fluorescence microscope (DM RXA; Leica, Cambridge, UK) and Leica Q600 Qwin V01.06 software. Pictures of all organs were taken using a fixed exposure time and were further processed identically.

Pharmacokinetics and biodistribution studies. A single dose of 0.3 μmol [^{3}H]COE-labeled Ab_{Esel} liposomes or IgG liposomes was injected intravenously at the onset of glomerulonephritis in C57bl/6 mice (n = 3/treatment group). Blood was sampled at 10 min, 60 min, 2 h, 6 h, and 24 h after injection. Blood was centrifuged, plasma was separated, and ^{3}H radioactivity was measured by a Packard Tri-Carb 2500 TR liquid scintillation analyzer (PerkinElmer Life And Analytical Sciences, Waltham, MA). The total amount of radioactivity in the plasma was calculated from the equation: plasma volume (ml) = [body wt (g)/1,000] × 78 × 0.56, where 78 is the mean blood volume of a mouse (ml/kg) and 0.56 is the relative amount of plasma based on a mean value for hematocrit in mice of 44 (vol%). Pharmacokinetic parameters were calculated according to population analysis using the Interactive Two-Stage Bayesian program (25). At 24 h, mice were killed, and organs were perfused with ice-cold PBS. Liver, spleen, kidney, lung, and heart were removed and processed for measurement of radioactivity as described previously (18).

Immunohistochemical and immunofluorescent detection of E-selectin and localization of intravenously injected Ab_{Esel} and immunoliposomes. Organ cryosections (5 μm) were fixed in acetone for 10 min and incubated for 45 min with MES-1 (10 μg/ml PBS). Endogenous biotin was blocked by a Biotin Blocking System (DakoCytomation Denmark), and peroxidase activity was blocked by incubation with 0.1% H_2O_2 in PBS for 10 min. Subsequently, sections were incubated for 1 h with biotin-labeled rabbit anti-rat antibodies (dilution 1:300 in PBS; DakoCytomation Denmark) in the presence of 5% normal mouse serum and 5% normal sheep serum and incubated for 30 min with streptavidin-avidin-biotin complex-HRP (DakoCytomation Denmark). Peroxidase activity was detected with 3-amino-9-ethylcarbazole (Sigma-Aldrich Chemie), and sections were counterstained with Mayer's hematoxylin. Isotype-matched controls were consistently found to be devoid of staining. Immunohistochemical staining of intravenously injected Ab_{Esel} (30 μg) and immunoliposomes (0.3 μmol lipid dose) was performed with biotin-labeled rabbit anti-rat antibodies on cryosections (n = 3/treatment group). Immunofluorescence double staining was performed for immunoliposomes and CD31. Endogenous biotin was blocked as described above. Ab_{Esel} and IgG liposomes were detected with Alexa $Fluor_{546}$-conjugated goat anti-rat antibodies (1-h incubation, 20 μg/ml PBS; Molecular Probes, Leiden, The Netherlands). CD31 [platelet endothelial cell adhesion molecule (PECAM)-1] was detected with biotin-labeled rat anti-mouse CD31 (clone 390, 5 μg/ml PBS; eBioscience, San Diego, CA), followed by Alexa $Fluor_{488}$-conjugated streptavidin (50 μg/ml PBS; Molecular Probes). All incubation steps were carried out in the presence of 5% normal mouse serum and 5% normal sheep serum. Sections were mounted with citifluor (Agar Scientific, Stansted, UK) and examined with a confocal scanning laser microscope (True

Confocal Scanner SP2 AOBS; Leica, Heidelberg, Germany) equipped with argon and neon lasers and coupled to a Leica DM IRE2 microscope using a HCX PL APO CS 63 × 1.40 oil immersion objective. Images were recorded by sequential scanning of the Alexa $Fluor_{488}$ and Alexa $Fluor_{546}$ signals to avoid bleedthrough of either signal in the recording channel of the other signal. Alexa $Fluor_{488}$ was recorded at λ_{ex} = 488 nm and λ_{em} = 500–535 nm, whereas Alexa $Fluor_{546}$ was recorded at λ_{ex} = 543 nm and λ_{em} = 555–700 nm. Both signals were recorded in the linear range, avoiding local saturation, and at an image resolution of 1,024 × 1,024 pixels. A series of 10 images was recorded along the *z*-axis from top to bottom of the tissue slice, and the final image was taken from a single plane in the middle of the tissue slice.

Pharmacological studies of Dexa-Ab_{Esel} liposome and free dexamethasone. For pharmacological effects, dexamethasone (25 μg/mouse; n = 4; Genfarma, Maarsen, The Netherlands), Dexa-IgG liposomes (0.4 μmol lipid, 25 μg dexamethasone phosphate; n = 3), and Dexa-Ab_{Esel} liposomes (0.4 μmol lipid, 25 μg dexamethasone phosphate; n = 6) were injected intravenously at the onset of glomerulonephritis induction. Mice were killed after 2 h, and kidneys were perfused with ice-cold PBS, harvested, snap-frozen in liquid nitrogen, and stored at −80°C before laser dissection microscopy and gene expression analysis. For collection of urine, mice were placed at *day 7* for 24 h in individual metabolic cages (n = 5–6/treatment group). Urinary albumin content was measured in 96-well microplates (NalgeNUNC International, Rochester, NY) with the mouse albumin enzyme-linked immunosorbent assay quantitation kit (Bethyl Laboratories, Montgomery, TX) using purified mouse albumin as a reference.

Laser dissection microscopy of renal microvascular endothelium. Seven hundred glomeruli (area 3 × 10^6 μm^2) and endothelial cells from arterioles (area 6 × 10^5 μm^2) and postcapillary venules (area 1 × 10^6 μm^2) were dissected from 5-μm cryosections using the Laser Robot Microbeam System (P.A.L.M. Microlaser Technology, Bernried, Germany) as described previously (2). Glomeruli were dissected through the Bowmans capsule so only cells within the glomeruli were catapulted away from the tissue. Arterioles and postcapillary venules were identified based on their morphology, and the inner layer of endothelial cells was dissected from the tissue.

Gene expression analysis. Total RNA was isolated from ten 8-μm cryosections with the RNeasy mini kit (Qiagen Benelux, Venlo, The Netherlands) including a DNase treatment on the column. For heart tissue, proteinase K (Qiagen) digestion was included as described by the manufacturer. RNA integrity was studied by standard laboratory methods. Extraction of total RNA from microdissected samples and DNase treatment were performed with the StrataPrep total RNA microprep kit (Stratagene Europe, Amsterdam, The Netherlands). RNA was reverse transcribed using SuperscriptIII reverse transcriptase (Invitrogen, Breda, The Netherlands) and random hexamer primers (Promega, Leiden, The Netherlands). Quantitative PCR amplifications were performed in duplicate according to the manufacturer's protocol on an ABI Prism 7900HT Sequence Detection System (Applied Biosystems, Applera Nederland, Nieuwerkerk a/d IJssel, The Netherlands). Relative gene expression of P-selectin (assay no.: Mm00441295_m1), E-selectin (Mm00441278_m1), and VCAM-1 (Mm00449197_m1) were calculated based on the expression of the housekeeping gene glyceraldehyde-3-phosphate dehydrogenase (Mm99999915_g1) according to the comparative cycle threshold (C_t) method ($\Delta C_t = C_{t\ \text{gene of interest}} - C_{t\ \text{housekeeping gene}}$). Microdissected samples from arterioles and postcapillary venules should contain endothelial cells only. To correct for possible contaminations of adjacent nonendothelial cells, gene expression was normalized to the constitutive expression of the endothelial marker gene CD31 (Mm00476702_m1), which was not influenced by the experimental conditions. Results were expressed as $2^{-\Delta C_{t\ \text{gene}}}/2^{-\Delta C_{t\ \text{CD31}}}$, which represents the relative amount of mRNA expressed, corrected for the amount of endothelial cells presented in each microdissected sample.

Statistic analysis. Statistical significance of differences was studied by means of the two-sided Student's *t*-test, assuming equal variances. Differences were considered to be significant when $P < 0.05$.

RESULTS

Ab_{Esel} liposomes bind specifically to activated mouse endothelial cells in vitro. Mouse endothelial cells abundantly expressed E-selectin when activated for 4 h with TNF-α (Fig. 1, *a* and *b*). The parental rat anti-mouse Ab_{Esel} bound to TNF-α-activated cells (Fig. 1, *c* and *d*) and maintained its binding quality when conjugated with liposomes (Fig. 1, *f* and *g*). Both Ab_{Esel} and Ab_{Esel} liposomes were taken up by activated endothelial cells, whereas no association of Ab_{Esel} or Ab_{Esel} liposomes was detected with quiescent, E-selectin negative cells. The specificity of the binding of Ab_{Esel} and Ab_{Esel} liposomes to E-selectin was further verified by competition with excess of unlabeled Ab_{Esel} antibodies (Fig. 1, *e* and *h*). Control rat IgG liposomes did not bind to endothelial cells (data not shown).

Upregulation of E-selectin on glomerular endothelium at the onset of glomerulonephritis. The classical accelerated anti-GBM glomerulonephritis model described by Assmann et al. (3) was slightly modified by including TNF-α in the anti-GBM antibody injection (2). This resulted in deposition of anti-GBM antibodies in a linear pattern along the capillary wall [Supplemental Fig. S1 (supplementary data for this article are available online at the *American Journal of Physiology: Renal Physiology* website)] and fast and reproducible inflammation in the glomeruli as demonstrated by a strong upregulation of E-selectin mRNA in laser microdissected glomeruli (Fig. 2*A*). Gene expression analysis in other organs showed a lower upregulation of E-selectin mRNA at 2 h in lungs, heart, and spleen that had returned to its basal level at 24 h. Upregulation

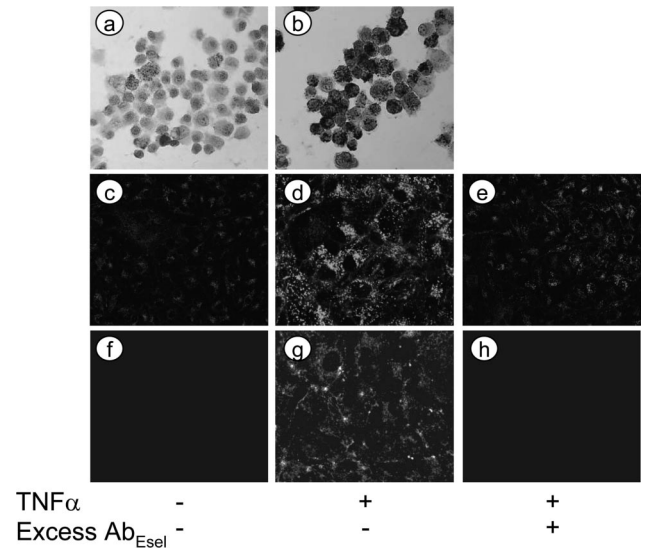

Fig. 1. Fluorescently labeled Ab_{Esel} and Ab_{Esel} liposomes associate with activated mouse endothelial cells. Immunohistochemical staining of E-selectin on cytospots of nonstimulated (*a*) and 4 h tumor necrosis factor (TNF)-α-stimulated (*b*) H5V. Binding and/or uptake of fluorescently labeled $Alexa_{488}$-Ab_{Esel} in nonstimulated (*c*) and 4 h TNF-α-stimulated (*d*) H5V. Association of fluorescently 1,1′-dioctadecyl-3,3,3′,3′-tetramethyl indocarbocyanine perchlorate (DiI)-labeled Ab_{Esel} liposomes in nonstimulated (*f*) and 4 h TNF-α-stimulated (*g*) H5V. Excess amount of nonlabeled Ab_{Esel} prevented cell association of $Alexa_{488}$-Ab_{Esel} (*e*) and DiI-labeled Ab_{Esel} (*h*) liposomes in TNF-α-stimulated H5V.

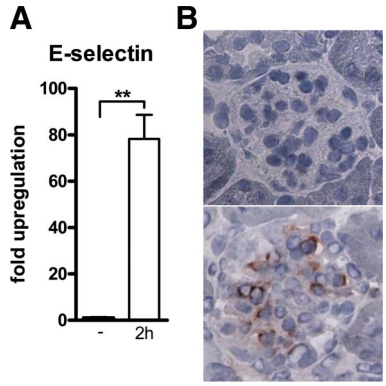

Fig. 2. Glomerular expression of E-selectin after induction of glomerulonephritis. *A*: upregulation of E-selectin mRNA 2 h after glomerulonephritis induction ($n = 9$ mice) determined in microdissected glomeruli. Average expression levels of E-selectin in glomeruli of untreated mice ($n = 4$) were arbitrarily set at one. Values are presented as means ± SE. $^{**}P < 0.001$. *B*: E-selectin protein is absent in the kidney of untreated mice (*top*) and present in the glomeruli of mice at 2 h after glomerulonephritis induction (*bottom*).

of E-selectin mRNA in liver was similar to the glomerular expression pattern (Supplemental Fig. S2). Upregulation of E-selectin gene expression in glomeruli was accompanied by expression of E-selectin protein at 2 h that was not detectable in untreated mice (Fig. 2*B*). Also at 24 h after glomerulonephritis induction, E-selectin protein was detected in glomeruli but not in heart, lung, liver, or spleen (Supplemental Fig. S3). At 2 h, a weak E-selectin staining was observed in all organs, probably because of short-lived systemic effects of TNF-α.

Pharmacokinetic behavior of Ab_{Esel} and IgG modified liposomes. Immunoliposomes were injected intravenously at the onset of glomerulonephritis induction. Plasma concentration of immunoliposomes decreased in a biphasic pattern (Fig. 3*A*). Plasma clearance and volume of distribution (area under the curve) of IgG liposomes were approximately twofold higher than those of Ab_{Esel} liposomes (Table 1). The initial plasma half-life $t(1)$ of Ab_{Esel} liposomes was longer than that of IgG liposomes, but no significant difference was observed between the mean terminal plasma half-lives $t(2)$ of the two immunoliposomes.

At 24 h, the tissue distribution of the immunoliposomes was analyzed in major organs (Fig. 3*B*). The targeting ratio, defined as the amount of Ab_{Esel} liposomes per gram tissue divided by the amount of IgG liposomes per gram tissue, was 3.6 in the kidney, by far the highest of all organs. The accumulation of both immunoliposomes in the spleen and lungs was not significantly different, whereas in the liver IgG liposomes accumulated to a higher extent. In the heart, accumulation of Ab_{Esel} liposomes was slightly higher than that of IgG liposomes, although this uptake was still low (≤0.2% of injected dose).

Immunolocalization of intravenously administered Ab_{Esel} antibodies and Ab_{Esel} liposomes. Immunohistochemical analysis was performed to visualize the localization of Ab_{Esel} antibodies and Ab_{Esel} liposomes throughout the body at 2 and 48 h after intravenous administration. Corroborating our results that in the kidney E-selectin protein was only expressed on glomerular endothelial cells (2), Ab_{Esel} and Ab_{Esel} liposomes homed to glomeruli in glomerulonephritis-induced mice (Fig. 4). Some association of Ab_{Esel} liposomes was observed with cells in the red pulp in the spleen and, based on morphological

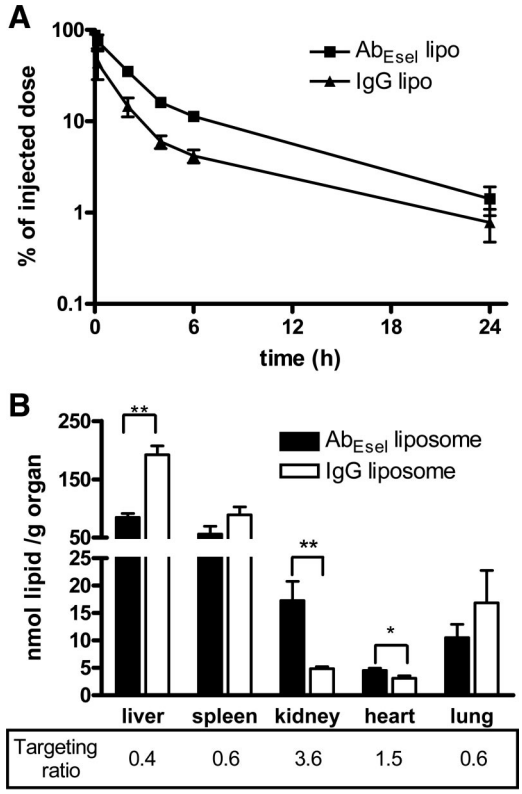

Fig. 3. Plasma disappearance and tissue distribution of Ab_{Esel} liposomes and control IgG liposomes. [^{3}H]cholesteryloleyl ether-labeled immunoliposomes were injected at the onset of glomerulonephritis. *A*: plasma disappearance measured at 10 min, 2 h, 4 h, 6 h, and 24 h. *B*: tissue distribution after 24 h. Nos. at *bottom* indicate targeting ratio (Ab_{Esel} liposomes/IgG liposomes). Values are presented as means ± SD; $n = 3$/group. $^*P < 0.05$ and $^{**}P < 0.01$.

appearance of the stained cells, with Kupffer cells in the liver, which reflects the regular elimination route of immunoliposomes from the body. After 48 h, Ab_{Esel} liposomes were still readily detectable in the kidney, whereas in spleen and liver the liposomes were not observed anymore. No immunoreactivity of Ab_{Esel} liposomes was seen in the heart. The parental Ab_{Esel} antibodies were not detected in organs other than the kidney, neither at 2 nor at 48 h. In untreated control mice, Ab_{Esel} antibodies were not detected in the kidney. Weak staining was observed for Ab_{Esel} liposomes in control animals, but noteworthy the staining was not specific for glomeruli (Fig. 4).

Ab_{Esel} liposomes but not IgG liposomes home to glomerular endothelium. In the kidney, glomerular immunostaining of intravenously injected Ab_{Esel} liposomes was stronger than that of IgG liposomes (Fig. 5*A*). To analyze the cellular location of

Table 1. *Pharmacokinetic parameters of immunoliposomes*

Parameter	Ab_{Esel} Liposomes	IgG Liposomes
AUC, h·%·ml^{-1}	280±26	137±14*
C_L, ml/h	16±1	32±3*
V_{ss}, ml/kg	97±4	200±29*
$t_{1/2}(1)$, h	0.98±0.05	0.64±0.02*
$t_{1/2}(2)$, h	6.24±0.81	7.18±0.93

Values represent mean values ± SD of 3 mice/group. AUC, area under the curve; C_L, plasma clearance; V_{ss}, steady-state volume of distribution; $t_{1/2}(1)$, initial half-life; $t_{1/2}(2)$, terminal half-life. $^*P < 0.05$.

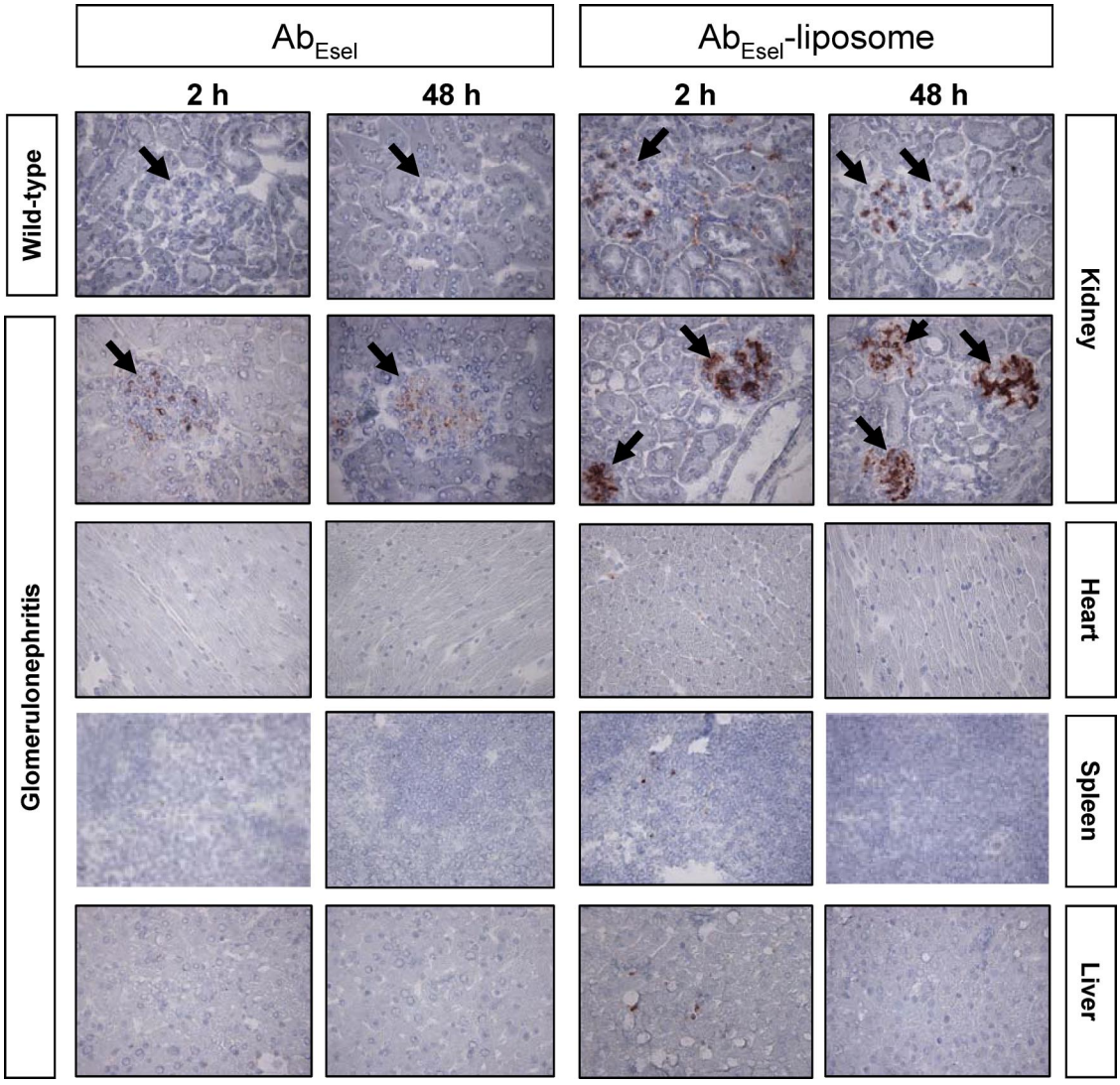

Fig. 4. Immunohistochemical detection of Ab_{Esel} antibodies and Ab_{Esel} liposomes injected iv in untreated mice and at the onset of glomerulonephritis. Mice were killed at 2 and 48 h (representative images from 3 mice/group). In kidney, Ab_{Esel} antibodies (*left*) and Ab_{Esel} liposomes (*right*) were detected in glomeruli of diseased animals. Extraglomerular vascular association was not observed. Ab_{Esel} was not detected in heart, spleen, or liver. Weak staining of Ab_{Esel} liposomes was observed in heart, spleen, and liver at 2 h after glomerulonephritis induction, but not after 48 h. Ab_{Esel} antibodies were not detected in untreated wild-type mice, whereas the staining of Ab_{Esel} liposomes was weak and not exclusive for glomeruli. Arrow indicates glomerulus.

both immunoliposomes within the glomeruli, immunofluorescent double staining was performed for immunoliposomes and the endothelial marker CD31 (PECAM-1). These analyses demonstrated colocalization of Ab_{Esel} liposomes with CD31-positive cells in the glomeruli, in contrast to IgG liposomes (Fig. 5*B*). As a result of glomerular endothelial uptake of Ab_{Esel} liposomes, but not IgG liposomes, E-selectin gene expression in the kidney was downregulated by Dexa-Ab_{Esel} liposomes but not by Dexa-IgG liposomes (Fig. 5*C*).

Dexa-Ab_{Esel} liposomes exert local pharmacological effects in glomeruli. Corticosteroids, including dexamethasone, have strong and pleiotropic anti-inflammatory effects, predominantly because of inhibition of proinflammatory gene expression. Combined with its rapid distribution to all cells in the body, its application is associated with severe side effects (4). This can be avoided by site-specific delivery of the drug. We asked the questions if targeted delivery of dexamethasone in glomerular endothelial cells by Ab_{Esel} liposomes exerted pharmacological effects locally in the glomeruli and if these effects were sufficient to switch off the inflammatory response of the kidney. Mice were killed 2 h after induction of glomerulonephritis, at which time point proinflammatory genes were robustly upregulated in the kidney (Fig. 6*A*). mRNA expression levels of proinflammatory cell adhesion molecules were compared in laser-microdissected glomeruli and renal arteriolar- and postcapillary venular endothelium, allowing analysis of site-specific pharmacological effects. Both free dexamethasone and Dexa-Ab_{Esel} liposomes significantly inhibited gene expression of P- and E-selectin and VCAM-1 in glomeruli (Fig. 6*B*). Analysis of the gene expression of VCAM-1 in microdissected renal arterioles and postcapillary venules showed that Dexa-Ab_{Esel} liposomes did not downregulate VCAM-1 expression, whereas free dexamethasone inhibited VCAM-1 expression by 70% (Fig. 6*C*). Arteriolar and venular E-selectin expression was below detection limits of quantitative RT-PCR analysis,

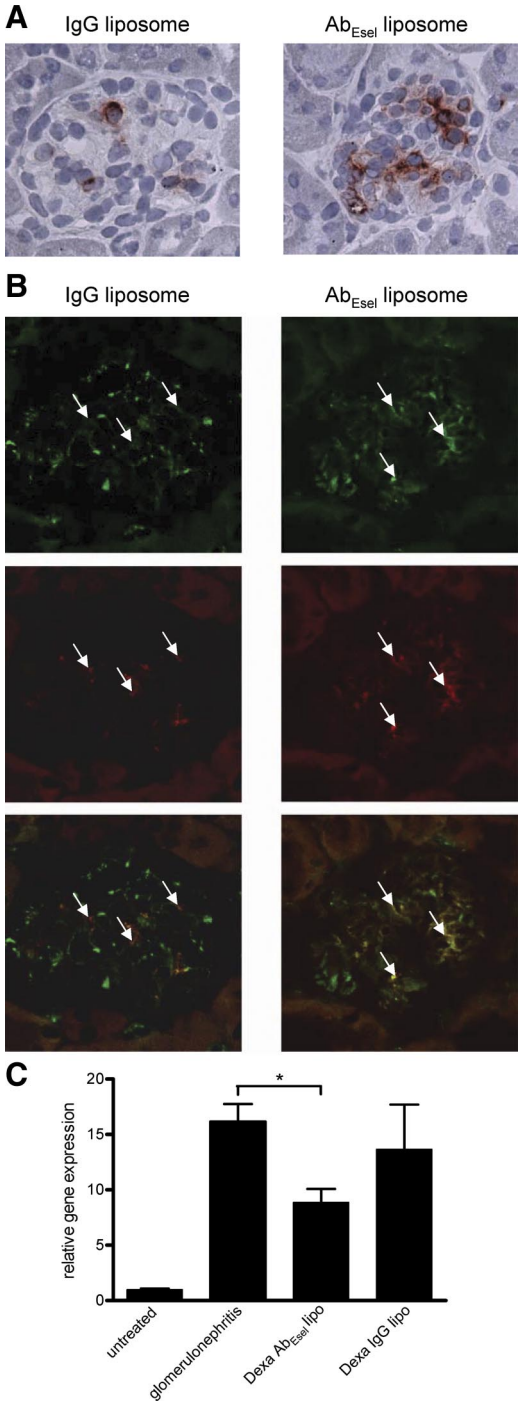

Fig. 5. Glomerular accumulation and cellular location differ for Ab$_{Esel}$ liposomes and IgG liposomes. *A*: immunodetection of Ab$_{Esel}$ liposomes and IgG liposomes in glomeruli. *B*: confocal microscopic images of double immunofluorescent staining demonstrated colocalization (yellow) of CD31 (green) with Ab$_{Esel}$ liposomes (red) but not with IgG liposomes (red). *C*: Dexa-Ab$_{Esel}$ liposomes, but not Dexa-IgG liposomes, reduced E-selectin gene expression in the kidney 2 h after glomerulonephritis induction. Average gene expression level in untreated mice was arbitrarily set at one. Values are presented as means ± SE; $n = 3$–6/group. *$P < 0.05$.

and no significant disease-mediated upregulation was observed for P-selectin in arterioles. In postcapillary venules, P-selectin was downregulated significantly by free dexamethasone and not by Dexa-Ab$_{Esel}$ liposomes (data not shown).

To analyze whether local downregulation of glomerular proinflammatory genes resulted in improved kidney function, 24-h urine samples were collected at *day 7* after initiation of glomerulonephritis development. A single injection at *day 0* of Dexa-Ab$_{Esel}$ liposomes significantly reduced albuminuria, whereas empty Ab$_{Esel}$ liposomes were devoid of effects (Fig. 6*D*). From this, we concluded that albuminuria reduction was not brought about by liposomal binding to glomerular endothelium per se but associated with drug delivery. Urine albumin levels in mice treated once with free dexamethasone were wide-ranging but not significantly different from untreated mice suffering from glomerulonephritis.

DISCUSSION

This study demonstrates that liposomes modified with E-selectin-specific monoclonal antibodies as a homing device selectively accumulated in glomerular endothelium in anti-GBM glomerulonephritis. The selectivity of the homing to glomerular endothelium was based on disease-induced site-selective expression of E-selectin on glomerular endothelium. The targeted local delivery of dexamethasone prevented proinflammatory gene expression in glomerular endothelium and did not affect gene expression in other renal (micro)vasculatures. The glomerular pharmacological effects were sufficient to improve renal function, as evidenced by diminished albuminuria.

Anti-GBM crescentic glomerulonephritis is treated with immunotherapy, consisting of glucocorticoids, cytotoxic drugs, and plasma exchange (28). The clinically important anti-inflammatory effects of glucocorticoids, however, are accompanied by systemic side effects. This stresses the importance of new, effective, and safe treatment strategies for glomerulonephritis (16). One way to increase drug efficacy is to selectively deliver the therapeutic entity into the diseased tissue. The focus of the current study was on targeted delivery of dexamethasone in glomerular endothelium. Because of the pivotal role of endothelial cells in the development and progression of glomerulonephritis and their good accessibility from the blood, they form a rational target for local pharmacological interference. The fundament for success of the glomerular endothelial drug targeting approach was the cell-type-specific expression of the target molecule E-selectin, an inflammation-induced, endothelial-specific protein (1). Restriction of E-selectin expression to endothelial cells has been shown to involve histone modifications of the promoter (9), although the molecular mechanisms for the heterogeneic control of endothelial E-selectin expression in different renal vascular beds are currently unknown.

Guided by disease-induced expression of E-selectin in glomerular endothelial cells, intravenously injected Ab$_{Esel}$ liposomes selectively accumulated in disease-affected glomeruli where they colocalized with endothelial cells. We calculated that, of the injected dexamethasone dose, when delivered by Ab$_{Esel}$ liposomes, 0.4 μg dexamethasone ends up in the kidney exclusively located in glomeruli, which constitute ~10% of kidney weight (27). Control IgG liposomes were also present in glomeruli, but to a fourfold lower extent and were not associated with endothelium. The glomerular presence of IgG liposomes in diseased animals can be explained by passive accumulation at the site of inflammation as a consequence of

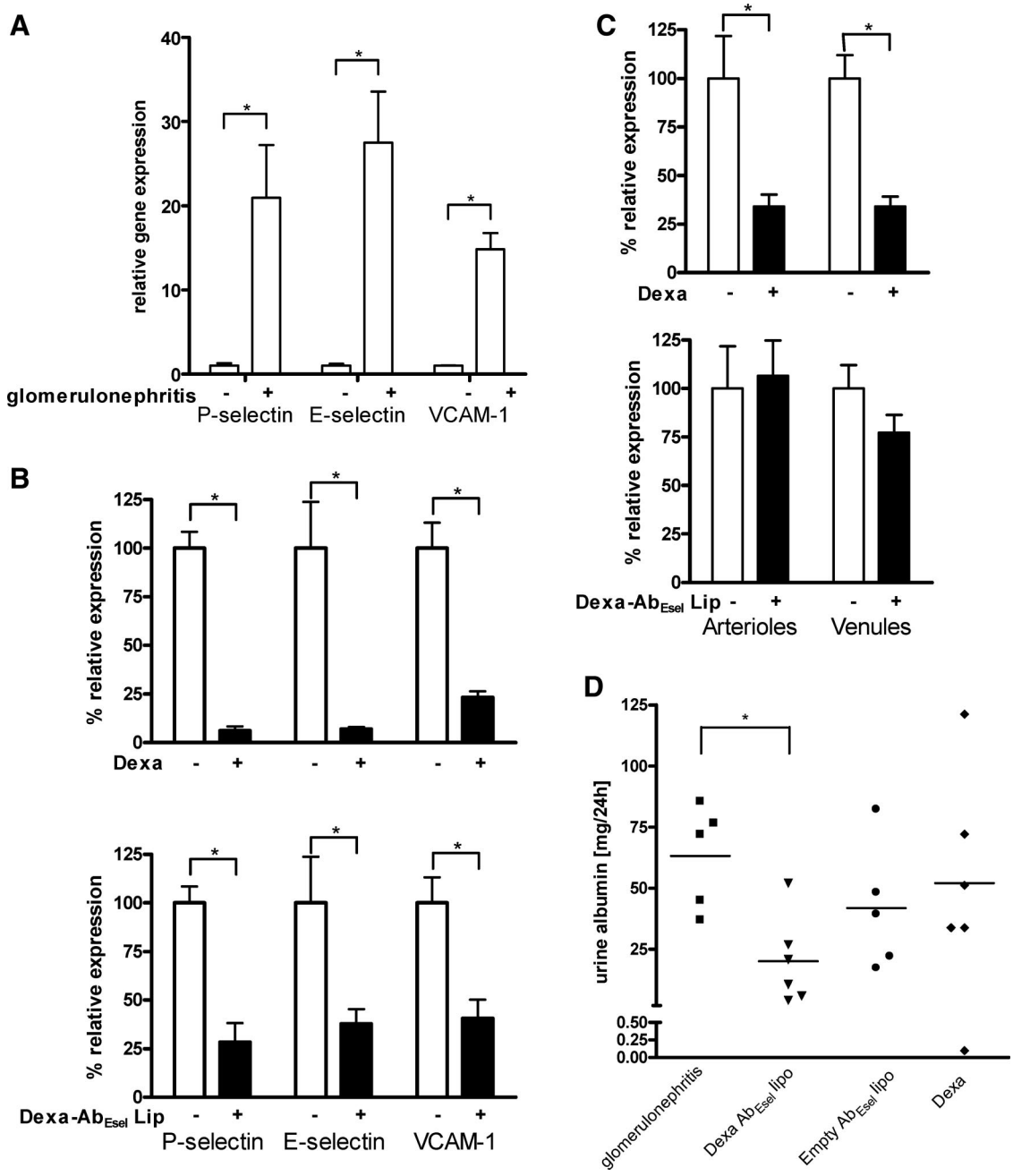

Fig. 6. Dexa-Ab_{Esel} liposomes downregulate gene expression of glomerulonephritis-induced endothelial cell adhesion molecules in glomerular endothelium only. *A*: gene expression of P-selectin, E-selectin, and vascular cell adhesion molecule (VCAM)-1 were upregulated in the kidney 2 h after induction of glomerulonephritis. Average gene expression level in untreated mice was arbitrarily set at one. *B*: dexamethasone (*top*) and Dexa-Ab_{Esel} liposomes (*bottom*) downregulated disease-induced P-selectin, E-selectin, and VCAM-1 expression in glomerular endothelium. *C*: dexamethasone (*top*) downregulated VCAM-1 in extraglomerular vascular beds. Dexa-Ab_{Esel} liposomes (*bottom*) did not have an effect on VCAM-1 expression in extraglomerular vascular beds. *B* and *C*: glomeruli, arterioles, and postcapillary venules were microdissected before quantitative RT-PCR. Gene expression levels in each vascular bed 2 h after induction of glomerulonephritis were arbitrarily set at 100%. Values are presented as means ± SE; $n = 3–6$/group. *D*: albuminuria at 7 days after glomerulonephritis induction was reduced significantly by Dexa-Ab_{Esel} liposomes. $*P < 0.05$.

enhanced permeability and retention, as has been demonstrated for nontargeted pegylated liposomes in an animal model of rheumatoid arthritis (22). IgG liposomes are possibly taken up by mesangial cells within glomeruli, because of their potent phagocytotic properties (20). The apparent discrepancy between detection of radioactive immunoliposomes in liver and spleen on one hand (Fig. 4), and lack of immunohistochemical detection in these organs on the other hand (Fig. 5), can be explained by rapid degradation of the antibody part of the immunoliposomes due to high proteolytic activity in macrophages and Kupffer cells (19). This explanation is further supported by the fact that Ab_{Esel} liposomes were weakly immunohistochemically detected in these organs at 2 h but not at all after 48 h.

The tool of laser capture microdissection in combination with quantitative RT-PCR enabled analysis of pharmacological

effects in endothelium of arteriolar, venous, and glomerular origin. We demonstrated vascular bed-specific effects that were masked when whole kidney homogenates were analyzed. We showed downregulation of glomerular expression of cell adhesion molecules as a consequence of targeted delivery of dexamethasone by Ab_{Esel} liposomes, whereas gene expression was unaltered in microvasculatures outside glomeruli. A single administration of Dexa-Ab_{Esel} liposomes was sufficient for reducing albuminuria 1 wk later. In a previous study, we showed that two weekly doses of Dexa-Ab_{Esel} liposomes resulted in improved renal functions at *day 14* (2). Our approach of glomerular endothelial-specific delivery of dexamethasone exerted a similar or even better pharmacological outcome than multicell type interference by an equimolar dose of free dexamethasone. When administered in its free form, dexamethasone distributes equally in the body and consequently has been shown to be present in all areas of the kidney (8). Apparently this generalized distribution of dexamethasone in the kidney does not lead to improved efficacy, whereas our data demonstrate that addressing only disease-affected endothelial cells that are primarily responsible for the inflammation leads to functional effects.

Immunoliposomal delivery of potent drugs in inflamed microvascular endothelium represents a new therapeutic strategy for glomerulonephritis. The approach described in this study may enable future applicability of many potent anti-inflammatory drugs that today do not make it through clinical trials because of severe side effects. The local and disease-specific expression of E-selectin on glomerular endothelium makes E-selectin an excellent target molecule for site-specific therapy. This strategy may be of clinical relevance for IgA nephropathy, lupus nephritis, and diabetic nephropathy, in which E-selectin expression was elevated in the kidney (14, 15).

ACKNOWLEDGMENTS

We thank Arjen Petersen for excellent assistance in animal experiments and Dr. Hans Proost for advice with regard to pharmacokinetic analysis.

GRANTS

This work was supported by Grants C01.1988 and C04.2080 from the Dutch Kidney Foundation (S. A. Ásgeirsdóttir, C. G. M. Kallenberg, and G. Molema) and by Vidi Grant 917.66.341 from the Dutch Organization of Scientific Research (P. Heeringa).

REFERENCES

1. **Aird WC.** Phenotypic heterogeneity of the endothelium: I. Structure, function, and mechanisms. *Circ Res* 100: 158–173, 2007.
2. **Asgeirsdottir SA, Kamps JA, Bakker HI, Zwiers PJ, Heeringa P, van der Weide K, Van Goor H, Petersen AH, Morselt H, Moorlag HE, Steenbergen E, Kallenberg CG, Molema G.** Site-specific inhibition of glomerulonephritis progression by targeted delivery of dexamethasone to glomerular endothelium. *Mol Pharmacol* 72: 121–131, 2007.
3. **Assmann KJ, Tangelder MM, Lange WP, Schrijver G, Koene RA.** Anti-GBM nephritis in the mouse: severe proteinuria in the heterologous phase. *Virchows Arch A Pathol Anat Histopathol* 406: 285–299, 1985.
4. **Barnes PJ.** How corticosteroids control inflammation: Quintiles Prize Lecture 2005. *Br J Pharmacol* 148: 245–254, 2006.
5. **Bartsch M, Weeke-Klimp AH, Meijer DK, Scherphof GL, Kamps JA.** Cell-specific targeting of lipid-based carriers for ODN and DNA. *J Liposome Res* 15: 59–92, 2005.
6. **Bottcher CDF, Van Gent CM, Pries C.** Rapid and sensitive submicro phosphorus determination. *Anal Chim Acta* 24: 203–204, 1961.
7. **Buttgereit F, Burmester GR, Lipworth BJ.** Optimised glucocorticoid therapy: the sharpening of an old spear. *Lancet* 365: 801–803, 2005.
8. **Coutard M, Osborne-Pellegrin MJ, Funder JW.** Tissue distribution and specific binding of tritiated dexamethasone in vivo: autoradiographic and cell fractionation studies in the mouse. *Endocrinology* 103: 1144–1152, 1978.
9. **Edelstein LC, Pan A, Collins T.** Chromatin modification and the endothelial-specific activation of the E-selectin gene. *J Biol Chem* 280: 11192–11202, 2005.
10. **Everts M, Schraa AJ, de Leij LFMH, Meijer DKF, Molema G.** Vascular endothelium in inflamed tissue as a target for site selective delivery of drugs. In: *Drug Targeting: Organ Specific Strategies*, edited by Molema G and Meijer DKF. New York: Wiley-VCH, 2001, p. 171–197.
11. **Everts M, Kok RJ, Asgeirsdottir SA, Melgert BN, Moolenaar TJ, Koning GA, van Luyn MJ, Meijer DK, Molema G.** Selective intracellular delivery of dexamethasone into activated endothelial cells using an E-selectin-directed immunoconjugate. *J Immunol* 168: 883–889, 2002.
12. **Falk RJ, Jenette JC, Nachmann PH.** Primary glomerular disease. In: *The Kidney*, edited by Brenner BM. Philadelphia PA: Saunders, 2004, p. 1293–1380.
13. **Garlanda C, Parravicini C, Sironi M, De Rossi M, Wainstok de Calmanovici R, Carozzi F, Bussolino F, Colotta F, Mantovani A, Vecchi A.** Progressive growth in immunodeficient mice and host cell recruitment by mouse endothelial cells transformed by polyoma middle-sized T antigen: implications for the pathogenesis of opportunistic vascular tumors. *Proc Natl Acad Sci USA* 91: 7291–7295, 1994.
14. **Hirata K, Shikata K, Matsuda M, Akiyama K, Sugimoto H, Kushiro M, Makino H.** Increased expression of selectins in kidneys of patients with diabetic nephropathy. *Diabetologia* 41: 185–192, 1998.
15. **Honkanen E, von Willebrand E, Teppo AM, Tornroth T, Gronhagen-Riska C.** Adhesion molecules and urinary tumor necrosis factor-alpha in idiopathic membranous glomerulonephritis. *Kidney Int* 53: 909–917, 1998.
16. **Javaid B, Quigg RJ.** Treatment of glomerulonephritis: will we ever have options other than steroids and cytotoxics? *Kidney Int* 67: 1692–1703, 2005.
17. **Kamps JA, Molema G.** Targeting liposomes to endothelial cells in inflammatory diseases. In: *Liposome Technology: Interactions of Liposomes with the Biological Milieu*, edited by Gregoriadis G. Boca Raton, FL: CRC, 2006, vol. III, p. 127–150.
18. **Kamps JAAM, Swart PJ, Morselt HWM, Pauwels R, de Béthune MP, De Clercq E, Meijer DKF, Scherphof GL.** Preparation and characterization of conjugates of (modified) human serum albumin and liposomes: drug carriers with an intrinsic anti-HIV activity. *Biochim Biophys Acta Biomembr* 1278: 183–190, 1996.
19. **Koning GA, Kamps JA, Scherphof GL.** Interference of macrophages with immunotargeting of liposomes. *J Liposome Res* 12: 107–119, 2002.
20. **Madsen KM, Tisher CC.** Anatomy of the kidney. In: *The* Kidney, edited by Brenner BM. Philadelphia, PA: Saunders, 2004, p. 3–72.
21. **Melgert BN, Olinga P, Jack VK, Molema G, Meijer DKF, Poelstra K.** Dexamethasone coupled to albumin is selectively taken up by rat non-parenchymal liver cells and attenuates LPS-induced activation of hepatic cells. *J Hepatol* 32: 603–611, 2000.
22. **Metselaar JM, Wauben MH, Wagenaar-Hilbers JP, Boerman OC, Storm G.** Complete remission of experimental arthritis by joint targeting of glucocorticoids with long-circulating liposomes. *Arthritis Rheum* 48: 2059–2066, 2003.
23. **Peifer C, Wagner G, Laufer S.** New approaches to the treatment of inflammatory disorders small molecule inhibitors of p38 MAP kinase. *Curr Top Med Chem* 6: 113–149, 2006.
24. **Peterson GL.** A simplification of the protein assay method of Lowry et al. which is more generally applicable. *Anal Biochem* 83: 346–356, 1977.
25. **Proost JH, Eleveld DJ.** Performance of an iterative two-stage bayesian technique for population pharmacokinetic analysis of rich data sets. *Pharm Res* 23: 2748–2759, 2006.
26. **Spragg DD, Alford DR, Greferath R, Larsen CE, Lee KD, Gurtner GC, Cybulsky MI, Tosi PF, Nicolau C, Gimbrone MA.** Immunotargeting of liposomes to activated vascular endothelial cells: a strategy for site-selective delivery in the cardiovascular system. *Proc Natl Acad Sci USA* 94: 8795–8800, 1997.
27. **Takemoto M, Asker N, Gerhardt H, Lundkvist A, Johansson BR, Saito Y, Betsholtz C.** A new method for large scale isolation of kidney glomeruli from mice. *Am J Pathol* 161: 799–805, 2002.
28. **Tam FW.** Current pharmacotherapy for the treatment of crescentic glomerulonephritis. *Expert Opin Investig Drugs* 15: 1353–1369, 2006.
29. **Vestweber D.** Regulation of endothelial cell contacts during leukocyte extravasation. *Curr Op Cell Biol* 14: 587–593, 2002.